GLIA 47:346–357 (2004)

Unique Distributions of the Gap Junction Proteins Connexin29, Connexin32, and Connexin47 in Oligodendrocytes

KLEOPAS A. KLEOPA,[1,2]* JENNIFER L. ORTHMANN,[1] ALAN ENRIQUEZ,[1] DAVID L. PAUL,[3] AND STEVEN S. SCHERER[1]

[1]*Department of Neurology, University of Pennsylvania Medical Center, Philadelphia, Pennsylvania*
[2]*Department of Clinical Neurosciences, Cyprus Institute of Neurology and Genetics, Nicosia, Cyprus*
[3]*Department of Neurobiology, Harvard Medical School, Boston, Massachusetts*

KEY WORDS Charcot-Marie-Tooth disease; neuropathy; myelin

ABSTRACT Oligodendrocytes of adult rodents express three different connexins: connexin29 (Cx29), Cx32, and Cx47. In this study, we show that Cx29 is localized to the inner membrane of small myelin sheaths, whereas Cx32 is localized on the outer membrane of large myelin sheaths; Cx29 does not colocalize with Cx32 in gap junction plaques. All oligodendrocytes appear to express Cx47, which is largely restricted to their perikarya. Cx32 and Cx47 are colocalized in many gap junction plaques on oligodendrocyte somata, particularly in gray matter. Cx45 is detected in the cerebral vasculature, but not in oligodendrocytes or myelin sheaths. This diversity of connexins in oligodendrocytes (in different populations of cells and in different subcellular compartments) likely reflects functional differences between these connexins and perhaps the oligodendrocytes themselves.

INTRODUCTION

Mutations in *GJB1*, the gene encoding the gap junction protein connexin32 (Cx32), cause X-linked Charcot-Marie-Tooth disease (CMTX), an inherited demyelinating neuropathy (http://molgen-www.uia.ac.be/CMTMutations/). Although Cx32 is highly expressed in both Schwann cells and oligodendrocytes (Dermietzel et al., 1990; Bergoffen et al., 1993; Scherer et al., 1995), CNS involvement in CMTX patients is usually subclinical (Nicholson et al., 1998; Bähr et al., 1999). Overt clinical CNS manifestations, however, have been associated with certain *GJB1/Cx32* mutations (Bell et al., 1996; Bort et al., 1997; Panas et al., 1998, 2001; Marques et al., 1999; Kawakami et al., 2002; Lee et al., 2002; Paulson et al., 2002; Schelhaas et al., 2002; Hanemann et al., 2003; Taylor et al., 2003), raising the possibility that Cx32 has an essential functional role in oligodendrocytes.

The reason for clinical or subclinical CNS manifestations of certain Cx32 mutations remains unclear. In the CNS, Cx32 is localized to the perikarya/cell bodies and proximal processes of oligodendrocytes and may be restricted to subpopulations of myelinated axons (Scherer et al., 1995; Kunzelmann et al., 1997; Li et al., 1997; Rash et al., 2001). Early evidence for additional connexins in oligodendrocytes was provided by freeze-fracture electron microscopy (EM) studies showing gap junction-like particles between apposed paranodal membranes (Sandri et al., 1977), where Cx32 is usually absent (Scherer et al., 1995; Kunzelmann et al., 1997; Li et al., 1997; Rash et al., 2001). Although a number of studies reported expression of Cx45 in oligodendrocytes (Dermietzel et al., 1997; Kunzelmann et al., 1997; Pastor et al., 1998), mice expressing histological reporters in place of Cx45 did not display oligodendrocyte expression (Kumai et al., 2000). Two other gap junction

*Correspondence to: Kleopas A. Kleopa, Cyprus Institute of Neurology and Genetics, P.O. Box 23462, 1683 Nicosia, Cyprus. E-mail: kleopa@cing.ac.cy

Received 30 October 2003; Accepted 13 February 2004

DOI 10.1002/glia.20043

Published online 30 April 2004 in Wiley InterScience (www.interscience.wiley.com).

proteins have been subsequently found in oligodendrocytes. The first, connexin29 (Cx29), is expressed both by central and peripheral myelinating cells (Altevogt et al., 2002; Li et al., 2002; Nagy et al., 2003a). The second, connexin47 (Cx47), previously described as neuron-specific (Teubner et al., 2001), is not present in neurons but is instead restricted to myelinating glial cells (Menichella et al., 2003; Odermatt et al., 2003).

Cx32 mutations may cause a toxic gain of function in oligodendrocytes due to altered trafficking and/or accumulation in the endoplasmic reticulum or Golgi of the corresponding mutant protein (Omori et al., 1996; Deschênes et al., 1997; Oh et al., 1997; VanSlyke et al., 2000; Kleopa et al., 2002; Yum et al., 2002). Although the R142W mutant, which is localized to the Golgi, also causes intracellular retention of wild-type Cx32 (Scherer et al., 1999), interactions between the products of both *GJB1/Cx32* alleles is not a possible mechanism in vivo, as only one *Gjb1/cx32* gene is expressed in Schwann cells owing to random inactivation of the X chromosome (Scherer et al., 1998). Transdominant interactions with another connexin, however, is a distinct possibility (Rouan et al., 2001); this could cause mistrafficking of the other (wild-type) connexin (Scherer et al., 1999) or even other deleterious effects (Abrams et al., 2002). Because the hemichannels of gap junctions are hexamers of connexin molecules (Bruzzone et al., 1996), and because different connexins can form (heteromeric) hemichannels (Stauffer, 1995), dominant-negative effects could occur during oligomerization in the Golgi (Musil and Goodenough, 1993) or in the cell membrane. We therefore investigated the localization of Cx29, Cx32, Cx45, and Cx47 in adult rat CNS. We did not detect Cx45 in oligodendrocytes, whereas Cx29, Cx32, and Cx47 each had a unique distribution.

MATERIALS AND METHODS

Immunoblots

Adult wild-type rats and mice, as well as *cx29*-, *cx32*-, and *cx47*-null mice were euthanized. Tissues were immediately frozen in liquid nitrogen and stored at −80°C or lysed directly in ice-cold 50 mM Tris, pH 7.0, 1% SDS, and 0.017 mg/ml phenylmethylsulfonyl fluoride (Sigma, St. Louis, MO), followed by a brief sonication on ice with a dismembrator (Fisher Scientific, Houston, TX). Protein concentration was determined using the Bio-Rad kit (Bio-Rad Laboratories, Richmond, CA). After a 5- to 15-min incubation in loading buffer at room temperature (RT), 100 μg of protein lysate from each sample was loaded onto a 12% SDS-polyacrylamide gel, electrophoresed, and transferred to an Immobilon-polyvinylidene fluoride membrane (Millipore, Bedford, MA) over 1 h using a semidry transfer unit (Fisher Scientific). The blots were blocked (5% powdered skim milk and 0.5% Tween-20 in Tris-buffered saline) for 1 h at RT and incubated overnight at 4°C with affinity-purified rabbit antisera against Cx29 (diluted 1:5) (Altevogt et al., 2002) or Cx47 (diluted 1:10,000) (Menichella et al., 2003) or with a rabbit antiserum against Cx32 (diluted 1:1,000; Zymed, San Francisco, CA). After washing in blocking solution, the blots were incubated in peroxidase-coupled secondary antibodies (diluted 1:10,000; Jackson ImmunoResearch, West Grove, PA) for 1 h at RT, washed again, and visualized by enhanced chemiluminescence using the ECL reagent (Amersham, Arlington Heights, IL).

Immunocytochemistry

Unfixed adult rat olfactory bulb, cerebrum, brain stem and attached cerebellum, and spinal cord were embedded in OCT and immediately frozen in a dry ice-acetone bath. These CNS tissues were also embedded in OCT following brief fixation (30–60 min) in Zamboni's fixative (Zamboni and de Martino, 1967) and infiltration in 20% sucrose in phosphate buffer (PB) overnight. Ten micron thick cryostat sections were thaw-mounted on SuperFrost Plus glass slides (Fisher Scientific) and stored at −20°C. Sections were postfixed and permeabilized by immersion in −20°C acetone for 10 min, blocked at room temperature for at least 1 h in 5% fish skin gelatin containing 0.5% triton X-100 in PBS, and incubated 16–48 h at 4°C with various combinations of primary antibodies: rabbit anti-Cx29 (1:200; against a C-terminus fusion protein) (Altevogt et al., 2002), rabbit anti-Cx32 (1:200; Chemicon), rabbit anti-Cx47 (1:500) (Menichella et al., 2003), mouse anti-Cx32 (7C6.C7; 1:2) (Li et al., 1997), mouse anti-Cx45 (1:100; Chemicon), mouse anti–rat myelin-associated glycoprotein (MAG; clone 513; 1:100; Boehringer Mannheim), mouse anti-Caspr (1:50) (Poliak et al., 1999), Rip (1:10; Developmental Hybridoma Bank), mouse anti-NeuN (1:100; Chemicon), and rat anti-GFAP (1:10; Sigma). Staining with affinity-purified anti-Cx29 or anti-Cx47 antibodies produced identical results with the nonaffinity-purified antibodies. After incubating with the primary antibodies, the slides were washed and incubated with the appropriate fluorescein- and rhodamine-conjugated donkey cross-affinity-purified secondary antibodies (diluted 1:100; Jackson ImmunoResearch) for 1 h at RT. Slides were mounted with Vectashield (Vector Laboratories, Burlingame, CA) and imaged with epifluorescence TRITC and FITC optics on a Leica DMR light microscope equipped with a cooled Hamamatsu camera or with a Leica TCS laser scanning confocal microscope, followed by image manipulation with Adobe Photoshop.

Processing for peroxidase-coupled secondary antibodies was similar to that described above, except that the sections were treated with 0.1% peroxide in methanol for 30 min to eliminate endogenous peroxidase activity prior to incubation with the primary antibodies. The slides were developed with biotinylated goat anti–rabbit antibodies for 1 h at RT, then incubated with ABC reagent (Vector Laboratories) for 30 min at RT and washed. Development of the peroxidase reaction product was performed using 0.5 mg/ml diamino-

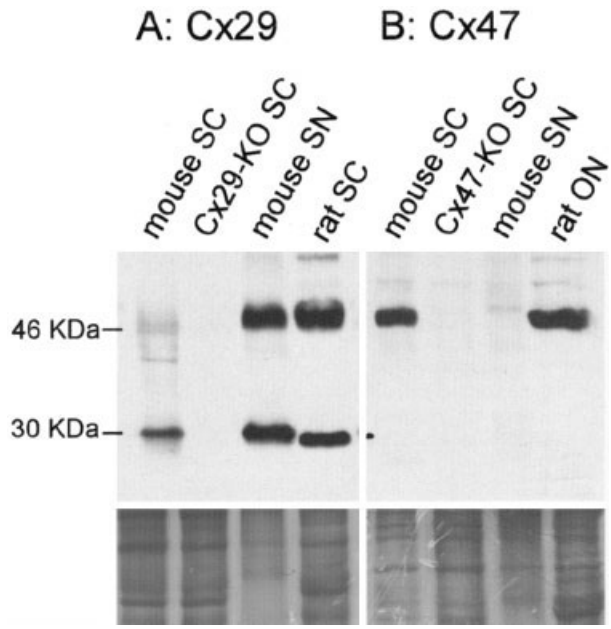

Fig. 1. Cx29 and Cx47 expression in neural tissues. These are immunoblots of the indicated tissues, hybridized with an affinity-purified rabbit antiserum against Cx29 (**A**) or Cx47 (**B**). The Cx29 antiserum (A) recognizes a ~ 30 kDa protein in wild-type mouse spinal cord (SC) and sciatic nerve (SN) as well as rat SC; this band is absent in *cx29*-null mouse spinal cord. A specific band around ~ 50 kDa is present in the same samples as Cx29, probably Cx29 dimers. The Cx47 antiserum (B) recognizes a ~ 46 kDa protein in wild-type mouse SC and rat optic nerve (ON); this band is absent both in *cx47*-null SC and in wild-type mouse SN. Images of the Commassie-stained gels are shown under the blots.

benzamine (Sigma) and 0.005% peroxide. Sections were imaged with bright-field optics and differential interference optics on a Leica DMR microscope equipped with a cooled Hamamatsu camera.

RESULTS

Antibody Characterization by Immunoblot

We have previously characterized the antibodies against Cx32; in *cx32/Gjb1*-null mice, they do not stain the sciatic nerves or CNS, nor do they recognize a band corresponding to Cx32 in immunoblots (Scherer et al., 1998; Abel et al., 1999). To evaluate the antisera against Cx29 (Altevogt et al., 2002) and Cx47 (Menichella et al., 2003), we hybridized blotted lysates from the spinal cords of *cx29*- and *cx47*-null mice as well as wild-type mice and rats. Antisera against Cx29 recognized a ~ 29 kDa band in wild-type spinal cord and mouse sciatic nerve but not in the Cx29 knockout spinal cord (Fig. 1A). In addition, there was a prominent band around 50 kDa in the mouse sciatic nerve and rat spinal cord samples, probably Cx29 dimers (Altevogt et al., 2002; Nagy et al., 2003a). The antiserum against Cx47 recognized a ~ 46 kDa band in wild-type mouse spinal cord and rat optic nerve, but not in the wild-type sciatic nerve or in the *cx47*-null spinal cord (Fig. 1B).

To ascertain that the pattern of Cx29 staining was authentic, we prepared longitudinal frozen sections of spinal cords from two adult *cx29*-null mice and a wild-type mouse. The sections were double-stained with a monoclonal antibody against Caspr and either a rabbit antiserum or an affinity-purified rabbit antiserum against Cx29. As shown in Figure 2, there was paranodal Caspr immunoreactivity in both the wild-type and the *cx29*-null samples, but no Cx29 immunoreactivity in the *cx29*-null samples. Further, the Cx29 immunostaining was most prominent in the juxtaparanodes (Fig. 2A) and perinuclear region of oligodendrocytes (Fig. 2B); no such staining was seen in *cx29*-null spinal cords (Fig. 2C and D). Finally, the Cx47 antisera did not appear to immunolabel cells in the CNS of *cx47*-null mice (data not shown). Thus, these antisera are specific.

Distribution of Cx32, Cx29, and Cx47 in CNS

We and others have previously shown that oligodendrocytes express Cx29, Cx32, and Cx47 (Scherer et al., 1995; Li et al., 1997; Altevogt et al., 2002; Li et al., 2002; Menichella et al., 2003; Odermatt et al., 2003). To compare the localization of these connexins in the adult CNS, we used peroxidase-conjugated secondary antibodies. In transverse sections of rat lumbar spinal cord (Fig. 3), Cx32 was predominantly expressed in the white matter, in the dorsal, lateral, and ventral funiculi (Scherer et al., 1995). This pattern is similar to that seen with antibodies that stain the components of compact myelin: proteolipid protein and myelin basic protein (Schwab and Schnell, 1989). Cx29, in contrast, was expressed more in gray matter and the corticospinal tract (Altevogt et al., 2002), both of which are enriched in small-diameter myelinated fibers (Arroyo et al., 2001). Cx47 staining was strongest in perikarya throughout the spinal cord, in white more than in the gray matter; myelinated axons per se were not heavily labeled. Cx32 and Cx29, but not Cx47, were strongly expressed in the spinal roots (Fig. 3). In agreement with Li and Simard (2001), we found Cx45 expression in cerebral blood vessels (data not shown), but not in oligodendrocytes (Dermietzel et al., 1997; Kunzelmann et al., 1997). These data demonstrate that Cx29, Cx32, and Cx47 each has distinct localizations in adult spinal cord.

Cx47 Is Expressed in Oligodendrocyte Perikarya

In order to clarify the cellular expression of Cx47, we used double labeling with markers for oligodendrocytes (Rip), astrocytes (GFAP), and neurons (NeuN) in different CNS areas. Cx47 was always localized in the perikaryon and proximal processes of cells both in the white and in the gray matter (Fig. 4). Staining with the oligodendrocyte marker Rip (Fig. 4A and data not shown) confirmed that almost all Cx47-positive cells also expressed Rip. Cx47 expression in other cell types

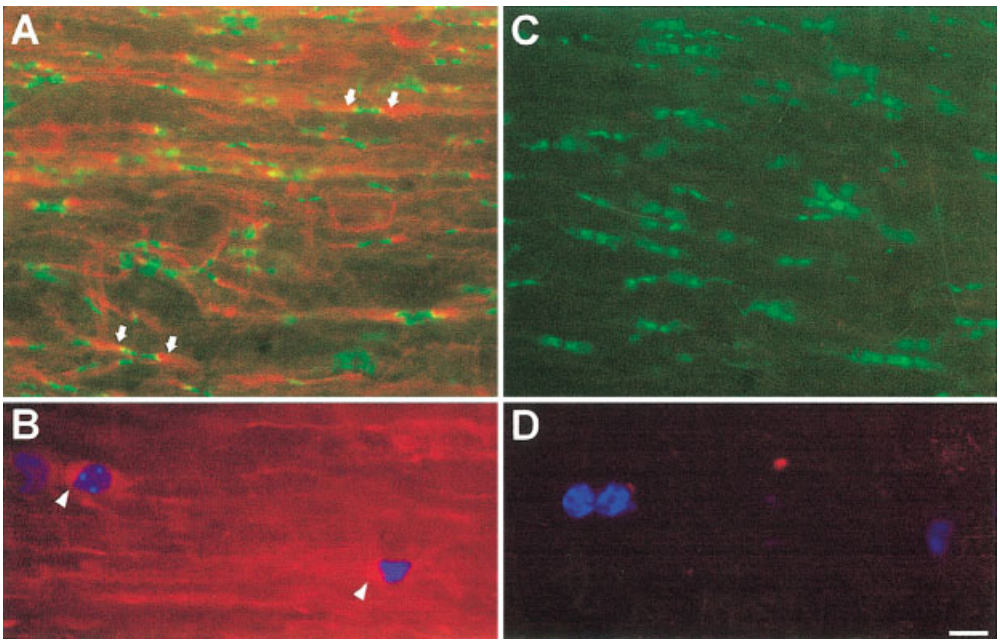

Fig. 2. Lack of Cx29 immunoreactivity in *cx29*-null mice. These are images of longitudinal sections of spinal cord from wild-type (**A** and **B**) and *cx29*-null (**C** and **D**) adult mice. The sections were immunostained with a rabbit antiserum against Cx29 (red) and a mouse monoclonal antibody against Caspr (green); DAPI (blue) was used as a nuclear counterstain. A and C show merged images of Cx29 and Caspr staining; B and D show merged images of Cx29 and DAPI staining. In every panel, each channel was exposed for a comparable amount of time and the images were not subsequently manipulated. Note the juxtaparanodal (arrows in A) and perinuclear (arrowheads in B) Cx29 staining in wild-type mice and the lack thereof in *cx29*-null mice (C and D). Scale bar = 10 μm.

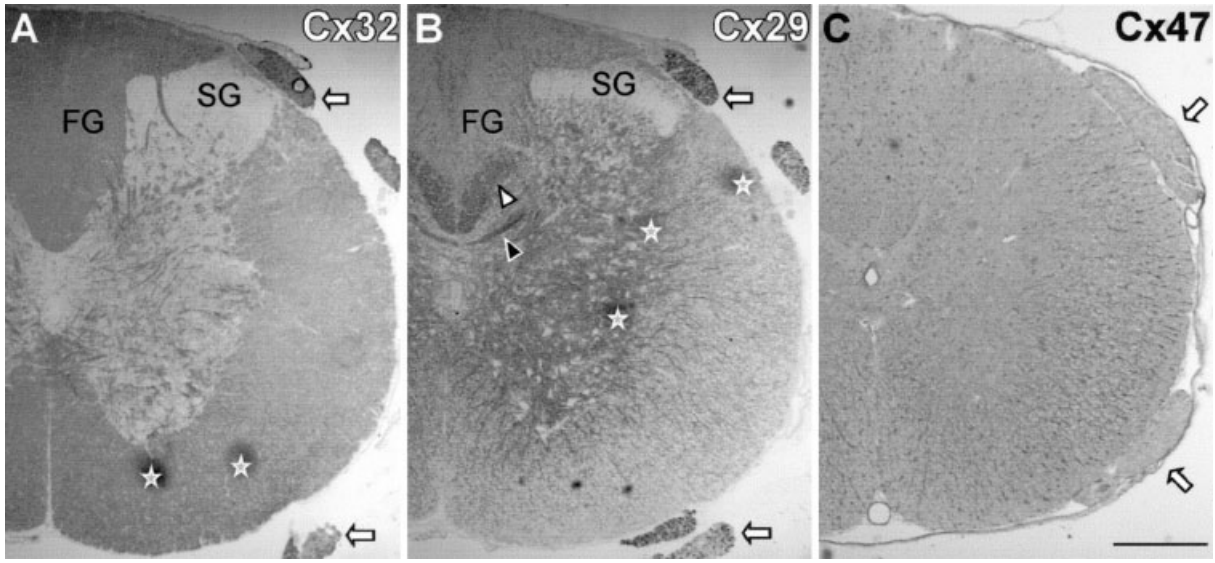

Fig. 3. Differential expression of Cx32, Cx29, and Cx47. These are images of transverse sections of unfixed (**A** and **B**) or Zamboni-fixed (**C**) adult rat lumbar spinal cord using rabbit antisera against Cx32 (A), Cx29 (B), and Cx47 (C), visualized with a peroxidase-conjugated secondary antiserum. Cx32 immunoreactivity is mainly found in white matter tracts. Cx29 immunoreactivity is stronger in the gray matter and in fiber tracts that are enriched in small diameter fibers including the crossing posterior commissural fibers (black arrowhead) and corticospinal fibers (white arrowhead). Cx47 immunoreactivity is mainly present in oligodendrocyte perikarya, which are more numerous in the white matter. Cx32 and Cx29, but not Cx47, are strongly expressed in the spinal roots (arrows). SG, substantia gelatinosa; FG, fasciculus gracilis. Asterisks mark artifactual areas of staining. Scale bar = 200 μm.

could not be excluded due to the fact that Rip stained the oligodendrocyte processes and myelin sheath, whereas Cx47 was mainly present at the perikaryon, often not directly colocalizing with Rip. However, double staining for Cx47 and either GFAP (Fig. 4B and data not shown) or NeuN (Fig. 4C and data not shown) demonstrated that Cx47-positive cells were never positive for either GFAP or NeuN, confirming that astrocytes and neurons do not express Cx47. Colocalization of Cx47 with Rip, in contrast to mu-

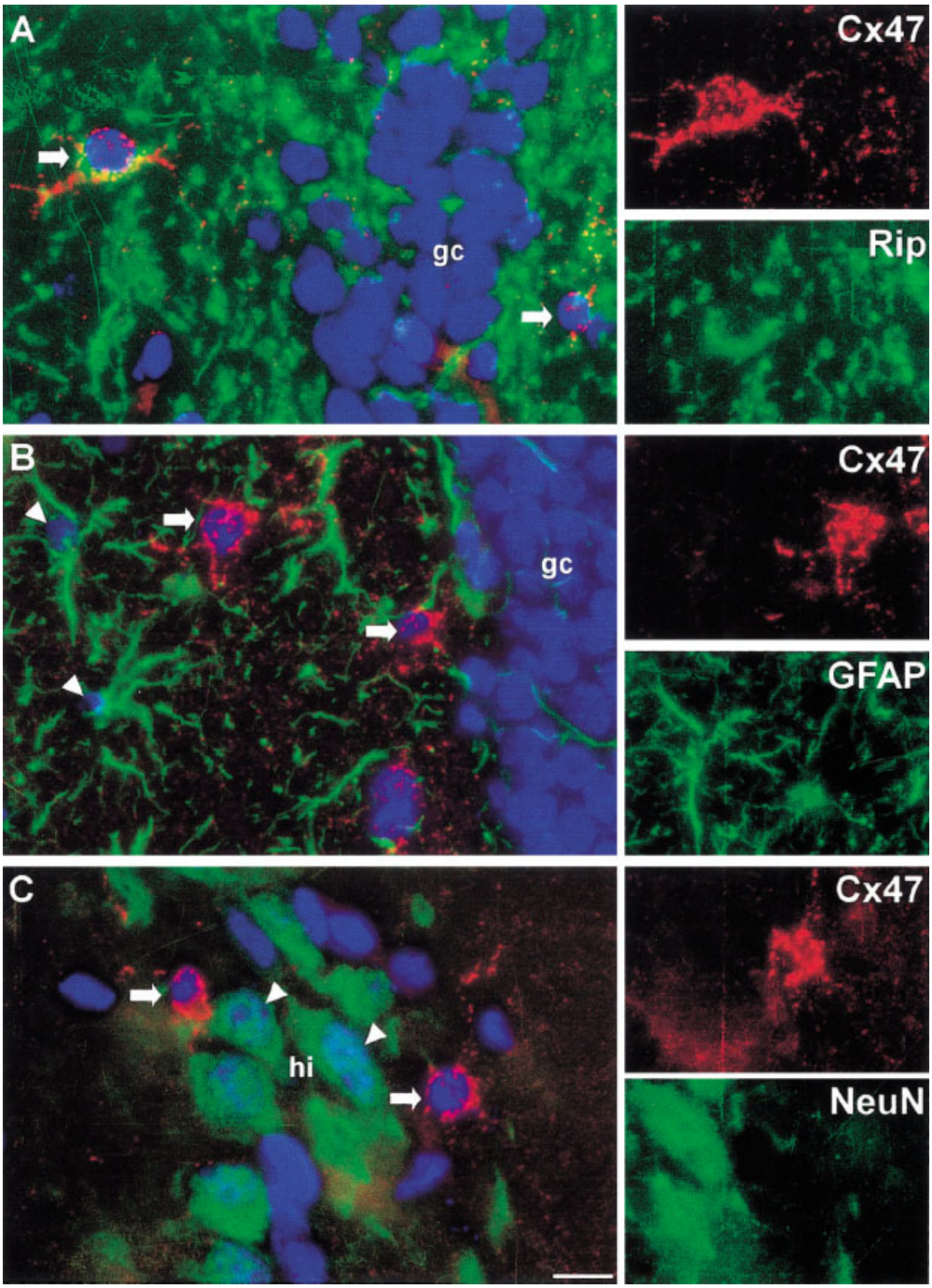

Fig. 4. Cx47 is expressed at the perikaryon of oligodendrocytes but not in astrocytes or neurons. These are images of sections of unfixed rat hippocampal dentate gyrus, immunostained for Cx47 (red) and either Rip (**A**), GFAP (**B**), or NeuN (**C**), markers for oligodendrocytes, astrocytes, and neurons, respectively (green). Nuclei are stained with DAPI (blue). Oligodendrocytes (arrows in A–C) express Cx47, whereas neurons in the granule cell layer (gc; A and B) or in the hilus region (hi; arrowheads in C) and astrocytes (arrowheads in B) do not. Scale bar = 10 μm.

tually exclusive expression of Cx47 and either GFAP or NeuN, was also demonstrated by confocal images (data not shown). In keeping with the immunoblot results, we could not detect any Cx47 expression in the peripheral nervous system by immunocytochemistry, either in the sciatic nerve or in the spinal roots (Fig. 3 and data not shown).

Cx29 Is Localized to Small Myelin Sheaths

To examine the localization of Cx29 in more detail, we labeled sections for Cx29 and Caspr, which is expressed at paranodes (Poliak et al., 1999), or MAG, which is localized on the adaxonal membrane (apposing the axon) of CNS myelin sheaths (Sternberger et al.,

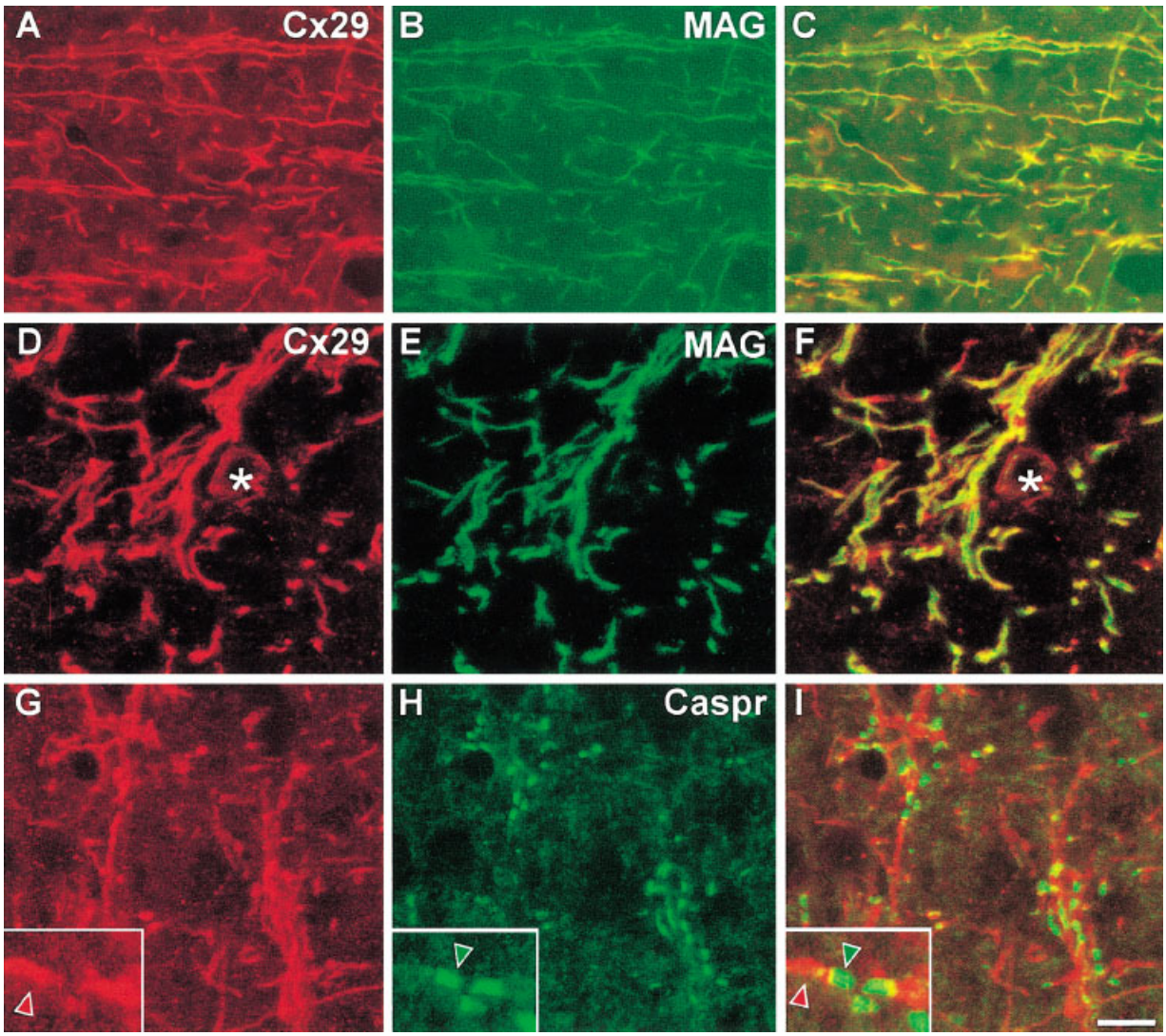

Fig. 5. Localization of Cx29 in small myelinated fibers. These are confocal images of unfixed sections of rat CNS, double-labeled with a rabbit antiserum against Cx29 (red) and a monoclonal antibody (green) against either MAG or Caspr, as indicated. Cx29 colocalizes with MAG along the myelin sheaths of small-caliber fibers in the superficial cortex (**A–C**) and in the olfactory bulb (**D–F**). Note the weakly Cx29-positive oligodendrocyte cell body (asterisk). In small myelinated axons of deep neocortex (**G–I**), Caspr (green arrows) is localized at the paranodes, whereas Cx29 (red arrows) is adjacent to Caspr in the juxtaparanodes (insets in higher magnification in G–I). Scale bar = 10 μm.

1979). As in the spinal cord (Fig. 2) (Altevogt et al., 2002), Cx29 was expressed at the juxtaparanodes of small- and medium-caliber fibers in the neocortex, adjacent to the Caspr-positive paranodes (Fig. 5G–I). In many small myelinated fibers, there was Cx29 staining along the entire internode, as shown by colocalization with MAG in the neocortex and olfactory bulb (Fig. 5A–F). We observed similar features in the small myelinated axons of optic nerves, striatum, pons, cerebellum, dorsal columns, and spinal cord gray matter (data not shown).

Expression of Cx29 in Relation to Cx32

To illuminate the relationship of Cx32 and Cx29 expression in the CNS, double labeling was performed in the same CNS regions. In the corpus callosum (CC), which contains mostly small myelinated axons (Sperber et al., 2001), there was robust Cx29 staining and little expression of Cx32 (Fig. 6A). The larger myelinated axons ventral to the CC, however, showed predominantly Cx32 expression and little Cx29 expression (Fig. 6A). The lateral olfactory tract (LOT), which also contains large myelinated axons, showed intense Cx32 immunoreactivity, in contrast to the adjacent white matter, which contains smaller Cx29-positive fibers (Fig. 6B). The large myelinated axons in the spinal cord dorsal columns were strongly Cx32-positive, whereas Cx29 was restricted to smaller-caliber myelinated axons and some oligodendrocytes (Fig. 6C). In the pons, the large Cx32-positive myelinated axons in the medial longitudinal fasciculus (MLF) were surrounded by

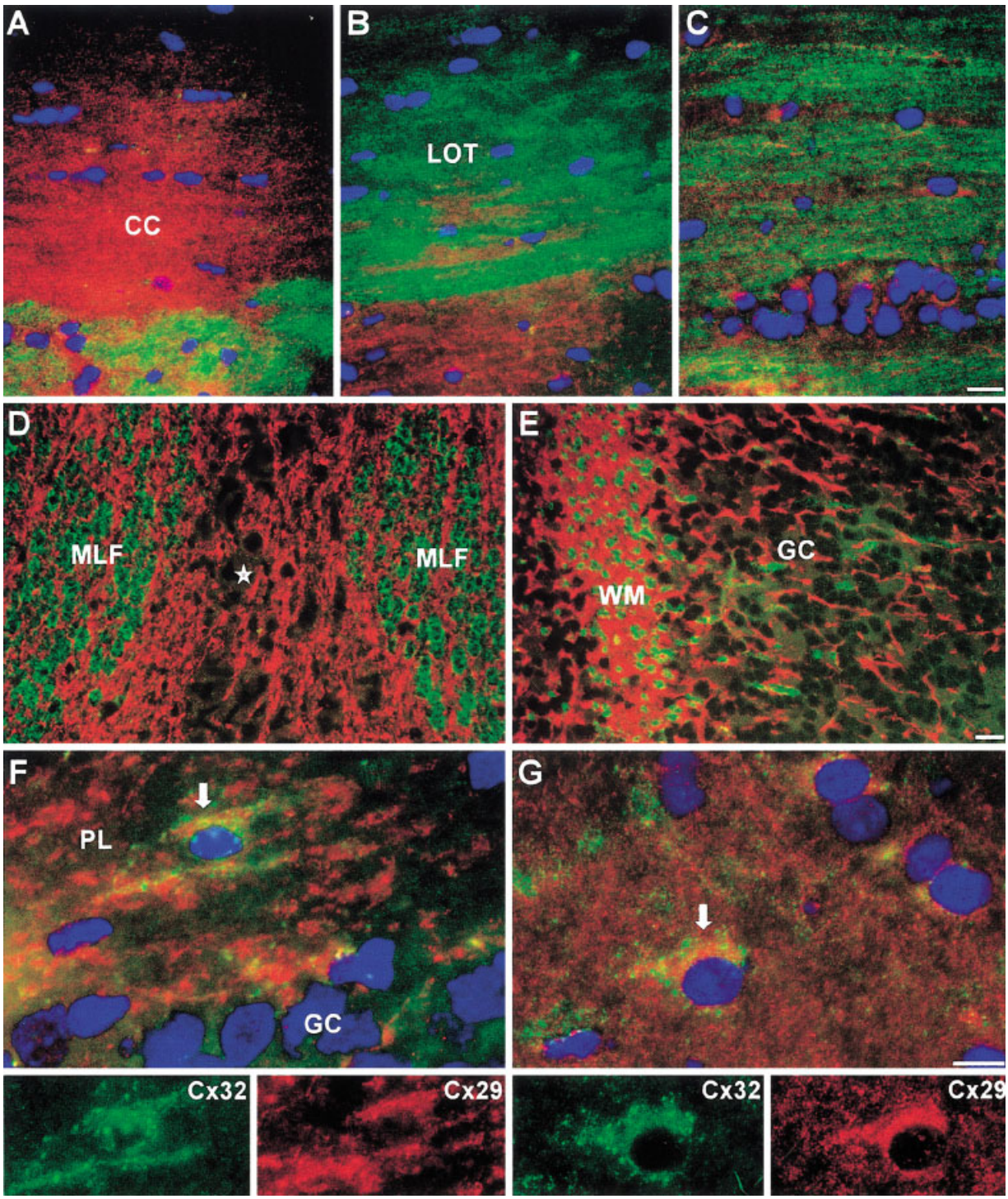

Fig. 6. The expression of Cx29 in relation to Cx32. These are images of unfixed rat CNS, immunostained with a rabbit antiserum to Cx29 (red) and a mouse monoclonal antibody against Cx32 (green), along with nuclear staining with DAPI (blue in A–C, F, and G). The expression of Cx29 and Cx32 was mutually exclusive in the white matter and partially overlapping in oligodendrocytes of the gray matter. In coronal sections through cerebrum (A and B), the small myelinated axons of the CC are mostly Cx29-positive, in contrast to the more ventral fibers, which are larger and Cx32-positive (**A**). The larger-diameter fibers in the LOT are Cx32-positive, in contrast to smaller, Cx29-positive fibers in the adjacent brain (**B**). In longitudinal sections of the spinal cord dorsal funiculus (**C**), Cx32 is present in large fibers, while Cx29 is restricted to some smaller fibers. In transverse sections of the pons (**D**), the large myelinated fibers of the MLF are Cx32-positive, whereas the surrounding smaller myelinated fibers are Cx29-positive (the midline is indicated by a star). In the cerebellum (**E**), smaller Cx29-positive fibers in the white matter (WM) adjacent to the granule cell layer (GC) surround larger Cx32-positive fibers. In the dentate gyrus of the hippocampus (**F**), an oligodendrocyte in the polymorphic layer (PL) adjacent to the GC expresses both Cx32 and Cx29 in the perikaryon and proximal processes (arrow). Similarly, in the spinal cord gray matter (**G**), the same cell (arrow) has Cx29 and Cx32 immunoreactivity. In both oligodendrocytes, however, Cx29 does not colocalize with Cx32 in gap junction-like plaques. Scale bars = 10 μm.

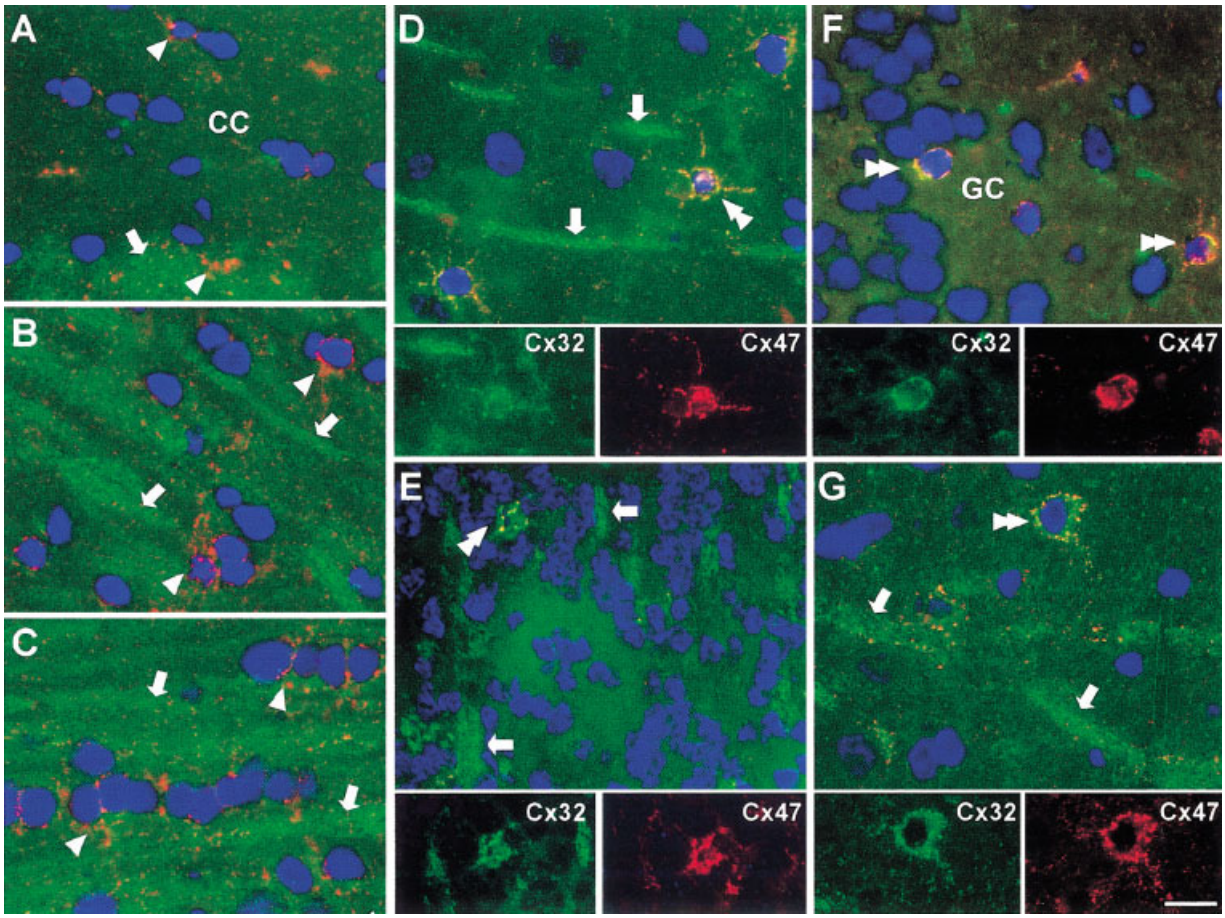

Fig. 7. Differential distribution of Cx32 and Cx47 in white and gray matter. These are images of unfixed rat CNS sections stained for Cx47 (red), Cx32 (green), and cell nuclei (blue). In the CC, Cx47 forms gap junction-like plaques (arrowhead) on the perikarya of oligodendrocytes (**A**). These perikarya and the surrounding small-diameter myelinated fibers have little Cx32 staining, whereas the myelinated fibers ventral to the CC are Cx32-positive (arrow). In the lateral olfactory tract (**B**) and spinal cord dorsal funiculus (**C**), Cx47 is expressed on the perikarya of interfascicular oligodendrocytes (arrowheads) that are surrounded by large, Cx32-positive myelinated fibers (arrows). In the deeper layers of neocortex (**D**), cerebellar granule cell layer (**E**), dentate gyrus of the hippocampus (**F**), and anterior horn of the spinal cord (**G**), Cx32 and Cx47 colocalize in some plaques on the perikarya and proximal processes of oligodendrocytes (double arrowheads). Note that oligodendrocytes myelinating Cx32-positive myelin sheaths (arrows in D, E, and G) appear to be directly connected to these oligodendrocyte perikarya. Scale bar = 10 μm.

smaller Cx29-positive fibers (Fig. 6D). In the cerebellar white matter, the more abundant Cx29-positive fibers surrounded the larger Cx32-positive fibers (Fig. 6E). The dichotomy in Cx29 and Cx32 expression between small and large myelinated fibers was also noted in the optic nerve, striatum, and olfactory bulb (data not shown).

In contrast to the white matter (Altevogt et al., 2002), Cx29 immunoreactivity was often found in gray matter oligodendrocytes (Nagy et al., 2003a). In the hippocampus, which is rich in small-diameter Cx29-positive fibers, Cx29 and Cx32 were typically coexpressed in oligodendrocyte perikarya (Fig. 6F). Even though the two connexins were coexpressed in the same cells, Cx29 was not found in the Cx32-positive plaques. The spinal cord gray matter (Fig. 6G) and other gray matter areas, including the neocortex and the olfactory bulb, showed similar patterns of Cx29 and Cx32 staining (data not shown). Thus, Cx29 does not appear to form typical gap junctions plaques on oligodendrocyte perikarya.

Expression of Cx47 in Relation to Cx32

To illuminate the relationship between these connexins in the white matter, double labeling was performed in multiple CNS regions as described above. In the CC (Fig. 7A), interfascicular oligodendrocytes were encrusted by Cx47-positive plaques, whereas there was little Cx32-immunostaining except in the more ventral, larger myelinated fibers (Fig. 5A). Similarly, in the LOT (Fig. 7B), dorsal columns (Fig. 7C), and MLF (data not shown), plaques of Cx47 immunoreactivity surrounded the perikarya of oligodendrocytes. The adjacent large-diameter myelinated fibers also expressed Cx32, but the oligodendrocyte perikarya themselves were typically Cx32-negative.

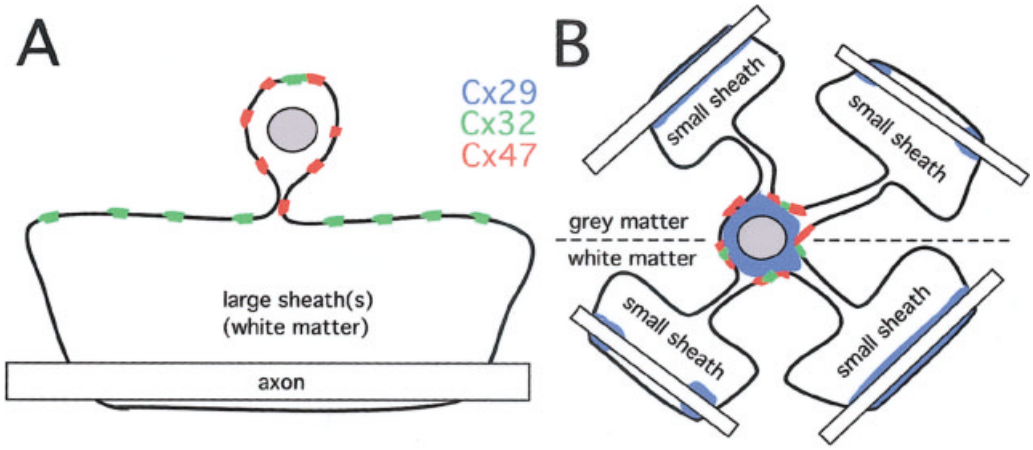

Fig. 8. The distribution of Cx29, Cx32, and Cx47 in oligodendrocytes. In this schematic drawing of two oligodendrocytes, the myelin sheaths have been unrolled to depict the localization of Cx29, Cx32, and Cx47. The oligodendrocyte myelinating the large axon (**A**) has numerous perikaryal gap junction plaques mainly comprised of Cx47 (red). Cx32 (green) is mainly expressed on the outer aspects of the myelin sheath, and Cx29 is absent. The oligodendrocyte myelinating small axons (**B**) has perikaryal gap junction plaques comprised of Cx47 (red) and Cx32 (green). Cx29 (blue) is localized to the perikaryal cytoplasm as well as the juxtaparanodal and internodal regions of the myelin sheath.

A different pattern was observed in the gray matter; Cx47 and Cx32 were colocalized in plaques on the perikarya and proximal processes. This was seen in regions that contained Cx32-positive myelin sheaths, such as the deep neocortex (Fig. 7D), cerebellar granule cell layer (Fig. 7E), anterior horn of the spinal cord (Fig. 7G), olfactory bulb (data not shown), and brainstem tegmentum (data not shown). Oligodendrocyte processes were observed extending to Cx32-positive myelin sheaths (Fig. 7D). In regions that were largely devoid of Cx32-positive myelin sheaths, such as the dentate gyrus of the hippocampus (Fig. 7F) and superficial neocortex (data not shown), Cx32 and Cx47 were typically present only at the perikaryon and proximal processes.

DISCUSSION

Oligodendrocytes Express Cx32, Cx29, and Cx47

Our results confirm and extend previous observations that oligodendrocytes express these three connexins. Each has a unique distribution at the subcellular level, as well as in different populations of oligodendrocytes, as summarized in Figure 8. Oligodendrocytes associated with the largest myelin sheaths, such as those in the MLF and the ventral funiculus of the spinal cord, have prominent Cx47-positive gap junction plaques on their perikaryal cell membrane (Menichella et al., 2003). Their proximal processes have gap junction plaques formed by Cx47 but also by Cx32, their myelin sheaths have Cx32 on their abaxonal (outermost) surface (Scherer et al., 1995; Rash et al., 2001; Menichella et al., 2003), but their adaxonal (inner) surface has little Cx29 (Altevogt et al., 2002). The oligodendrocyte perikarya associated with small myelin sheaths appear to have gap junction plaques comprised of Cx32 and Cx47; Cx29 is also expressed in the somata, but does not appear to form plaques. Small myelin sheaths have Cx29 in their adaxonal membrane, both at juxtaparanodes and internodes (Altevogt et al., 2002; Nagy et al., 2003a), but typically do not have detectable Cx32 or Cx47.

Distinct Oligodendrocyte Populations

Our findings extend our previous observations that different oligodendrocyte subpopulations express different connexins according to the caliber of the myelinated axon (Scherer et al., 1995; Altevogt et al., 2002): large myelinated fibers express Cx32, whereas small myelinated fibers express Cx29. Although Nagy et al. (2003a) recently reported that both connexins were present on large- and small-diameter fibers, the predominant expression of Cx32 in the former and of Cx29 in the latter is striking. These differences remain to be resolved. A similar distinction has been previously demonstrated for other molecules: oligodendrocytes associated with the smallest fibers express the carbonic anhydrase isoform II but not S-MAG, while those ensheathing the largest show the opposite pattern (Butt and Berry, 2000). Cx47, in contrast, seems to be widely expressed in the perikaryon and proximal processes, regardless of the size of the myelinated axon.

Since the original work of Del Rio-Hortega (1928), oligodendrocytes have been classified by their morphological features (Bunge, 1968; Friedman et al., 1989; Remahl and Hildebrand, 1990; Hildebrand et al., 1993; Berry et al., 1995; Ibrahim et al., 1995; Weruaga-Prieto et al., 1996; Butt and Berry, 2000). Type I and II are morphologically similar and populate the gray matter and discrete white matter tracts, including the optic nerve, corpus callosum, and corticospinal tracts. Each type I and II oligodendrocyte myelinates numerous small-diameter (below 2–4 μm) axons, and their mye-

lin sheaths are thin and short. Type III oligodendrocytes myelinate a small number of larger-diameter axons (above 2–4 μm), forming thicker myelin sheaths with longer internodes. Type IV oligodendrocytes are similar to type III, but have a cell body directly overlying the individual axon that they myelinate; they are typically found in white matter tracts containing large-diameter fibers, including the spinal cord fasciculi and the lateral olfactory tract. The myelin sheaths of individual type III and IV oligodendrocytes are about 50 times larger than those of type I/II oligodendrocytes (Remahl and Hildebrand, 1990; Hildebrand et al., 1993; Butt et al., 1998). In spite of these substantial differences, the phenotype of oligodendrocytes appears to be determined by the axons with which they associate in development (Fanarraga et al., 1998).

Gap Junction Proteins of Oligodendrocytes

The diversity of connexins, their different localizations, and their expression by subsets of oligodendrocytes suggest that each may serve a specialized role in oligodendrocytes. Cx32 and Cx47 overlap at least in part, as both appear to form gap junctions on somata of oligodendrocytes. This redundancy may be the reason that mice lacking Cx32 or Cx47 alone have minimal abnormalities in CNS myelin, whereas mice lacking both have profound CNS demyelination (Menichella et al., 2003; Odermatt et al., 2003). Such redundancy may also explain why subclinical abnormalities, such as delay in brainstem auditory-evoked potentials, are commonly found in patients with CMTX (Nicholson et al., 1998; Bähr et al., 1999), whereas dramatic, transient CNS phenotypes are associated with certain mutations (Panas et al., 2001; Paulson et al., 2002; Schelhaas et al., 2002; Taylor et al., 2003). We previously evaluated the possibility that some Cx32 mutants associated with CNS phenotypes have dominant interactions with Cx45, but found no evidence for such interactions (Kleopa et al., 2002). Now that it is clear that oligodendrocytes do not express Cx45, we are similarly evaluating possible interactions of Cx32 mutants with human Cx31.3, the human homolog of Cx29 (Altevogt et al., 2002) and especially Cx47.

In oligodendrocytes somata, we found that Cx29 is not associated with Cx32- or Cx47-positive plaques, in contrast to the report of Nagy et al. (2003a), who found Cx29 in much smaller gap junction plaques. In a subsequent study, these authors reported that Cx29 was sparse on oligodendrocyte somata, exhibited limited colocalization with Cx32 in these cells, and failed to display the pattern of punctate labeling characteristic of other connexins that play a role in the formation of astrocytic-oligodendrocytic gap junctions (Nagy et al., 2003b). Although Cx29 is colocalized with MAG, probably on the inner/adaxonal membrane of oligodendrocytes, it remains to be determined whether Cx29 forms hemichannels on the inner/adaxonal oligodendrocyte cell membrane, as we previously suggested (Altevogt et al., 2002). In our previous studies, Cx29 failed to form functional homotypic channels in vitro. However, this may not represent the in vivo situation, since the same study (Altevogt et al., 2002) suggested a modulating effect of Cx29 on Cx32 voltage gating. Other still unknown regulating factors may be required for the function of Cx29 channels in vivo, which are not present in vitro. Thus, the normal function of Cx29 in myelinating glial cells and its possible interactions with other connexins need to be clarified. Cx29 does not prevent the development of demyelination in *Gjb1/cx32*-null mice, even though it appears to be expressed in its normal pattern (data not shown). Further, the R142W Cx32 mutant, which is retained in the Golgi, does not affect the trafficking of Cx29 in myelinating Schwann cells in transgenic mice (data not shown). Whether Cx32 mutants interact with Cx29 in either Schwann cells or oligodendrocytes remains to be determined, but such interactions could modify the phenotype of CMTX.

Astrocyte-Oligodendrocyte Coupling

Freeze-fracture EM demonstrates that most, if not all, gap junctions formed by oligodendrocytes are with astrocytes, and are located at oligodendrocyte perikarya, their proximal processes, and the outer membrane of the myelin sheath (Massa and Mugnaini, 1982; Waxman and Black, 1984; Nagy et al., 1997; Rash et al., 2001). Cx32 and Cx47 are localized in a corresponding manner (Dermietzel et al., 1989; Scherer et al., 1995; Kunzelmann et al., 1997; Li et al., 1997; Rash et al., 2001; Menichella et al., 2003; Odermatt et al., 2003) and hence likely form these gap junction plaques, as has been recently shown in normal and Cx32 knockout mice (Nagy et al., 2003b). Because astrocytes express Cx26, Cx30, and Cx43 (Dermietzel et al., 1989; Kunzelmann et al., 1999; Nagy et al., 1999; Rash et al., 2001), and not Cx29, Cx32, or Cx47, the gap junctions between oligodendrocytes and astrocytes must be heterotypic, formed by hemichannels comprised of different connexins. Oligodendrocyte-astrocyte coupling may be complex, as each hemichannel may be comprised of more than one kind of connexin, and not all possible combinations of oligodendrocyte and astrocyte hemichannels are known to be compatible (Bruzzone et al., 1996) or spatially associated in situ (Nagy et al., 2003a). Finally, astrocytes themselves are extensively coupled by gap junctions, so oligodendrocyte-astrocyte coupling is a part of a "pan-glial synctium" (Massa and Mugnaini, 1982; Rash et al., 1997) whose functional attributes are still largely unexplored.

In addition to conventional intercellular junctions, oligodendrocytes may also establish reflexive gap junctions between adjacent paranodal loops (Sandri et al., 1977; Bergoffen et al., 1993; Scherer et al., 1995; Balice-Gordon et al., 1998), similar to the ones present in Schwann cells (Sandri et al., 1977; Bergoffen et al., 1993; Scherer et al., 1995; Balice-Gordon et al., 1998).

Whether Cx32 is present at CNS paranodes is not settled (Scherer et al., 1995; Li et al., 1997). Cx29 is the major gap junction protein in the paranodal region of the CNS, but it has not been found in the paranodal loops themselves (Altevogt et al., 2002; Li et al., 2002). Thus, it is possible that another connexin forms gap junctions between CNS paranodal loops.

ACKNOWLEDGMENTS

Supported by a National Multiple Sclerosis Society grant (RG3454A1/T to K.A.K.) and the National Institutes of Health (RO1 NS42878 to S.S.S. and RO1 GM37751 to D.L.P.).

REFERENCES

Abel A, Bone LJ, Messing A, Scherer SS, Fischbeck KF. 1999. Studies in transgenic mice indicate a loss of connexin32 function in X-linked Charcot-Marie-Tooth disease. J Neuropathol Exp Neurol 58:702–710.

Abrams C, Bennett M, Verselis V, Bargiello T. 2002. Voltage opens unopposed gap junction hemichannels formed by a connexin 32 mutant associated with X-linked Charcot-Marie-Tooth disease. Proc Natl Acad Sci USA 99:3980–3984.

Altevogt B, Kleopa K, Postma F, Scherer S, Paul D. 2002. Connexin29 is uniquely distributed within myelinating glial cells of the central and peripheral nervous systems. J Neurosci 22:6458–6470.

Arroyo EJ, Xu T, Poliak S, Watson M, Peles E, Scherer SS. 2001. Internodal specializations of myelinated axons in the CNS. Cell Tiss Res 305:53–66.

Bähr M, Andres F, Timmerman V, Nelis E, Van Broeckhoven C, Dichgans J. 1999. Central visual, acoustic, and motor pathway involvement in a Charcot-Marie-Tooth family with an Asn205Ser mutation in the connexin32 gene. J Neurol Neurosurg Psychiat 66:202–206.

Balice-Gordon RJ, Bone LJ, Scherer SS. 1998. Functional gap junctions in the Schwann cell myelin sheath. J Cell Biol 142:1095–1104.

Bell C, Willison H, Clark C, Haites N. 1996. CNS abnormalities in a family with a connexin32 mutation and peripheral neuropathy. Eur J Hum Genet 4:S136.

Bergoffen J, Scherer SS, Wang S, Oronzi-Scott M, Bone L, Paul DL, Chen K, Lensch MW, Chance P, Fischbeck K. 1993. Connexin mutations in X-linked Charcot-Marie-Tooth disease. Science 262: 2039–2042.

Berry M, Ibrahim M, Carlile J, Fuge F, Duncan A, Butt A. 1995. Axon-glial relationships in the anterior medullary velum of the adult rat. J Neurocytol 24:965–983.

Bort S, Nelis E, Timmerman V, Sevilla T, Cruz-Martinez A, Martinez F, Millan JM, Arpa J, Vilchez JJ, Prieto F, Van Broeckhoven C, Palau F. 1997. Mutational analysis of the MPZ, PMP22 and Cx32 genes in patients of Spanish ancestry with Charcot-Marie-Tooth disease and hereditary neuropathy with liability to pressure palsies. Hum Genet 99:746–754.

Bruzzone R, White TW, Paul DL. 1996. Connections with connexins: the molecular basis of direct intercellular signaling. Eur J Biochem 238:1–27.

Bunge R. 1968. Glial cells and the central myelin sheath. Physiol Rev 48:197–251.

Butt AM, Ibrahim M, Berry M. 1998. Axon-myelin sheath relations of oligodendrocyte unit phenotypes in the adult rat anterior medullary velum. J Neurocytol 27:259–269.

Butt A, Berry M. 2000. Oligodendrocytes and the control of myelination in vivo: new insights from the rat anterior medullary velum. J Neurosci Res 59:477–488.

Del Rio-Hortega P. 1928. Tercera aportacion al conocimiento morfologico e interpretacion functional de la oligodendroglia. Mem Real Soc Esp Hist Nat 14:5–122.

Dermietzel R, Traub O, Hwang TK, Beyer E, Bennett MVL, Spray DC, Willecke K. 1989. Differential expression of three gap junction proteins in developing and mature brain tissues. Proc Natl Acad Sci USA 86:10148–10152.

Dermietzel R, Hwang TK, Spray DS. 1990. The gap junction family: structure, function and chemistry. Anat Embryol 182:517–528.

Dermietzel R, Farooq M, Kessler JA, Althaus H, Hertzberg EL, Spray DC. 1997. Oligodendrocytes express gap junction proteins connexin32 and connexin45. Glia 20:101–114.

Deschênes SM, Walcott JL, Wexler TL, Scherer SS, Fischbeck KH. 1997. Altered trafficking of mutant connexin32. J Neurosci 17: 9077–9084.

Fanarraga ML, Griffiths IR, Zhao M, Duncan ID. 1998. Oligodendrocytes are not inherently programmed to myelinate a specific size of axon. J Comp Neurol 399:94–100.

Friedman B, Hockfield S, Black JA, Woodruff KA, Waxman SG. 1989. In situ demonstration of mature oligodendrocytes and their processes: an immunocytochemical study with a new monoclonal antibody, Rip. Glia 2:380–390.

Hanemann CO, Bergmann C, Senderek J, Zerres K, Sperfeld AD. 2003. Transient, recurrent, white matter lesions in X-linked Charcot-Marie-Tooth disease with novel connexin 32 mutation. Arch Neurol 60:605–609.

Hildebrand C, Remahl S, Persson H, Bjartmar C. 1993. Myelinated nerve fibres in the CNS. Prog Brain Res 40:319–384.

Ibrahim M, Butt A, Berry M. 1995. Relationship between myelin sheath diameter and internodal length in axons of the anterior medullary velum of the adult rat. J Neurol Sci 133:119–127.

Kawakami H, Inoue K, Sakakihara I, Nakamura S. 2002. Novel mutation in X-linked Charcot-Marie-Tooth disease associated with CNS impairment. Neurology 59:923–926.

Kleopa K, Yum S, Scherer S. 2002. Cellular mechanisms of connexin32 mutations associated with CNS manifestations. J Neurosci Res 68:522–534.

Kumai M, Nishii K, Nakamura K, Takeda N, Suzuki M, Shibata Y. 2000. Loss of connexin45 causes a cushion defect in early cardiogenesis. Development 127:3501–3512.

Kunzelmann P, Blumcke I, Traub O, Dermietzel R, Willecke K. 1997. Coexpression of connexin45 and -32 in oligodendrocytes of rat brain. J Neurocytol 26:17–22.

Kunzelmann P, Schroder W, Traub O, Steinhauser C, Dermietzel R, Willecke K. 1999. Late onset and increasing expression of the gap junction protein connexin30 in adult murine brain and long-term cultured astrocytes. Glia 25:111–119.

Lee M-J, Nelson I, Houlden H, Sweeney M, Hilton-Jones D, Blake J, Wood N, Reilly M. 2002. Six novel connexin32 (GJB1) mutations in X-linked Charcot-Marie-Tooth disease. J Neurol Neurosurg Psychiatry 73:304–306.

Li J, Hertzberg EL, Nagy JI. 1997. Connexin32 in oligodendrocytes and association with myelinated fibers in mouse and rat brain. J Comp Neurol 379:571–591.

Li X, Simard J. 2001. Connexin45 gap junction channels in rat cerebral vascular smooth muscle cells. Amer J Physiol Heart Circ Physiol 281:H1890–H1898.

Li X, Lynn B, Olson C, Meier C, Davidson K, Yasumura T, Rash J, Nagy J. 2002. Connexin29 expression, immunocytochemistry and freeze-fracture replica immunogold labelling (FRIL) in sciatic nerve. Eur J Neurosci 16:795–806.

Marques W, Sweeney MG, Wood NW, Wroe SJ, Marques W. 1999. Central nervous system involvement in a novel connexin 32 mutation affecting identical twins. J Neurol Neurosurg Psychiat 66:803–804.

Massa PT, Mugnaini E. 1982. Cell junctions and intramembrane particles of astrocytes and oligodendrocytes: a freeze-fracture study. Neuroscience 7:523–538.

Menichella D, Goodenough D, Sirkowski E, Scherer S, Paul D. 2003. Connexins are critical for normal myelination in the CNS. J Neurosci 23:5963–5973.

Musil LS, Goodenough DA. 1993. Multisubunit assembly of an integral plasma membrane channel protein, gap junction connexin43, occurs after exit from the ER. Cell 74:1075–1077.

Nagy JI, Ochalski PAY, Li J, Hertzberg EL. 1997. Evidence for the co-localization of another connexin with connexin-43 at astrocytic gap junctions in rat brain. Neuroscience 78:533–548.

Nagy JI, Patel D, Ochalski PAY, Stelmack GL. 1999. Connexin30 in rodent, cat and human brain: selective expression in gray matter astrocytes, co-localization with connexin43 at gap junctions and late developmental appearance. Neuroscience 88:447–468.

Nagy J, Ionescu A, Lynn B, Rash J. 2003a. Connexin29 and connexin32 at oligodendrocyte and astrocyte gap junctions and in myelin of the mouse central nervous system. J Comp Neurol 22:356–370.

Nagy J, Ionescu A, Lynn B, Rash J. 2003b. Coupling of astrocyte connexins Cx26, Cx30, Cx43 to oligodendrocyte Cx29, Cx32, Cx47: implications from normal and connexin32 knockout mice. Glia 44: 205–218.

Nicholson GA, Yeung L, Corbett A. 1998. Efficient neurophysiological selection of X-linked Charcot-Marie-Tooth families. Neurology 51: 1412–1416.

Odermatt B, Wellershaus K, Wallraff A, Seifert G, Degen J, Euwens C, Fuss B, Bussow H, Schilling K, Steinhauser C, Willecke K. 2003. Connexin 47 (Cx47)-deficient mice with enhanced green fluorescent protein reporter gene reveal predominant oligodendrocytic expression of Cx47 and display vacuolized myelin in the CNS. J Neurosci 23:4549–4559.

Oh S, Ri Y, Bennett MVL, Trexler EB, Verselis VK, Bargiello TA. 1997. Changes in permeability caused by connexin 32 mutations underlie X-linked Charcot-Marie-Tooth disease. Neuron 19:927–938.

Omori Y, Mesnil M, Yamasaki H. 1996. Connexin 32 mutations from X-linked Charcot-Marie-Tooth disease patients: functional defects and dominant negative effects. Mol Biol Cell 7:907–916.

Panas M, Karadimas C, Avramopoulos D, Vassilopoulos D. 1998. Central nervous system involvement in four patients with Charcot-Marie-Tooth disease with connexin 32 extracellular mutations. J Neurol Neurosurg Psychiat 65:947–948.

Panas M, Kalfakis N, Karadimas C, Vassilopoulos D. 2001. Episodes of generalized weakness in two sibs with the C164T mutation of the connexin 32 gene. Neurology 57:1906–1908.

Pastor A, Kremer M, Moller T, Kettenmann H, Dermietzel R. 1998. Dye coupling between spinal cord oligodendrocytes: differences in coupling efficiency between gray and white matter. Glia 24:108–120.

Paulson H, Garbern J, Hoban T, Krajewski K, Lewis R, Fischbeck K, Grossman R, Lenkinski R, Kamholz J, Shy M. 2002. Transient central nervous system white matter abnormality in X-linked Charcot-Marie-Tooth disease. Ann Neurol 52:429–434.

Poliak S, Gollan L, Martinez R, Custer A, Einheber S, Salzer JL, Trimmer J, Shrager P, Peles E. 1999. Caspr2, a new member of the neurexin superfamily is localized at the juxtaparanodes of myelinated axons and associates with K^+ channels. Neuron 24:1037–1047.

Rash JE, Duffy HS, Dudek FE, Bilhartz BL, Whalen LR, Yasumura T. 1997. Grid-mapped freeze-fracture analysis of gap junctions in gray and white matter of adult rat central nervous system, with evidence for a "panglial syncytium" that is not coupled to neurons. J Comp Neurol 388:265–292.

Rash JE, Yasumura T, Dudek FE, Nagy JI. 2001. Cell-specific expression of connexins and evidence of restricted gap junctional coupling between glial cells and between neurons. J Neurosci 21:1983–2000.

Remahl S, Hildebrand C. 1990. Relation between axons and oligodendroglial cells during initial myelination: 1, the glial unit. J Neurocytol 19:313–328.

Rouan F, White T, Brown N, Taylor A, Lucke T, Paul D, Munro C, Uitto J, Hodgins M, Richard G. 2001. Trans-dominant inhibition of connexin-43 by mutant connexin-26: implications for dominant connexin disorders affecting epidermal differentiation. J Cell Sci 114: 2105–2113.

Sandri C, Van Buren J, Akert K. 1977. Membrane morphology of the vertebrate nervous system: a study with freeze-etch technique. Prog Brain Res 46:1–384.

Schelhaas H, Van Engelen B, Gabreels-Festen A, Hageman G, Vliegen J, Van Der Knaap M, Zwarts M. 2002. Transient cerebral white matter lesions in a patient with connexin 32 missense mutation. Neurology 59:2007–2008.

Scherer SS, Deschênes SM, Xu Y-T, Grinspan JB, Fischbeck KH, Paul DL. 1995. Connexin32 is a myelin-related protein in the PNS and CNS. J Neurosci 15:8281–8294.

Scherer SS, Xu Y-T, Nelles E, Fischbeck K, Willecke K, Bone LJ. 1998. Connexin32-null mice develop a demyelinating peripheral neuropathy. Glia 24:8–20.

Scherer SS, Bone LJ, Abel A, Deschênes SM, Balice-Gordon R, Fischbeck K. 1999. The role of the gap junction protein connexin32 in the pathogenesis of X-linked Charcot-Marie-Tooth disease. In: Cardew G, editor. Gap junction-mediated intercellular signaling in health and disease. New York: John Wiley and Sons. p 175–185.

Schwab ME, Schnell L. 1989. Region-specific appearance of myelin constituents in the developing rat spinal cord. J Neurocytol 18:161–164.

Sperber BR, Boyle–Walsh EA, Engleka MJ, Gadue P, Peterson AC, Stein PL, Scherer SS, McMorris FA. 2001. A unique role for fyn in CNS myelination. J Neurosci 21:2039–2047.

Stauffer KA. 1995. The gap junction proteins β_1-connexin (connexin-32) and β_2-connexin (connexin-26) can form heteromeric hemichannels. J Biol Chem 270:6768–6772.

Sternberger NH, Quarles RH, Itoyama Y, Webster HD. 1979. Myelin-associated glycoprotein demonstrated immunocytochemically in myelin and myelin-forming cells of developing rat. Proc Natl Acad Sci USA 76:1510–1514.

Taylor RA, Simon EM, Marks HG, Scherer SS. 2003. The CNS phenotype of X-linked Charcot-Marie-Tooth disease: more than a peripheral problem. Neurology 61:1475–1478.

Teubner B, Odermatt B, Guldenagel M, Sohl G, Degen J, Bukauskas FF, Kronengold J, Verselis VK, Jung YT, Kozak CA, Schilling K, Willecke K. 2001. Functional expression of the new gap junction gene connexin47 transcribed in mouse brain and spinal cord neurons. J Neurosci 21:1117–1126.

VanSlyke JK, Deschênes SM, Musil LS. 2000. Intracellular transport, assembly, and degradation of wild-type and disease-linked mutant gap junction proteins. Mol Biol Cell 11:1933–1946.

Waxman SG, Black JA. 1984. Freeze-fracture ultrastructure of the perinodal astrocyte and associated glial junctions. Brain Res 308: 77–87.

Weruaga-Prieto E, Eggli P, Celio MR. 1996. Topographic variations in rat brain oligodendrocyte morphology elucidated by injection of lucifer yellow in fixed tissue slices. J Neurocytol 25:19–31.

Yum S, Kleopa K, Shumas S, Scherer SS. 2002. Diverse trafficking abnormalities of Connexin32 mutants causing CMTX. Neurobiol Dis 11:43–52.

Zamboni L, de Martino C. 1967. Buffered picric-acid formaldehyde: a new rapid fixative for electron-microscopy. J Cell Biol 35:148A.